The Chaotic Pendulum

Sanjana Gupta

PHY-2020-1: Physics Lab 3

Final Project

Instructor: Prof. Susmita Saha

Teaching Fellow: Chinkey

Teaching Assistants: Jagat Kafle, Spandan Pandya

6th May 2023

Abstract

This paper presents the results of an experimental study and simulations on the dynamics of various types of pendulums. The experimental data collected from the simple pendulum was analyzed using phase plots and Fourier transform, while the magnetic pendulum was analyzed using phase plots, Fourier transform, Lyapunov exponent, and bifurcation diagram to show that it exhibits chaotic behavior. Additionally, a damped driven pendulum was simulated, demonstrating that it exhibits chaotic behavior for certain parameters. By varying the damping constant, further insights were gained into the behavior of the damped driven pendulum. The results obtained in this study provide a deeper understanding of the dynamics of pendulums and their chaotic behavior.

Contents

1 Theoretical Background

1.1 Damped-Driven Pendulum

A system consisting of a bob, an inextensible string connected to a mechanical pivot is considered. The mechanical pivot rotates providing the system a sinusoidal driving force $F_0 cos\omega_d t$.

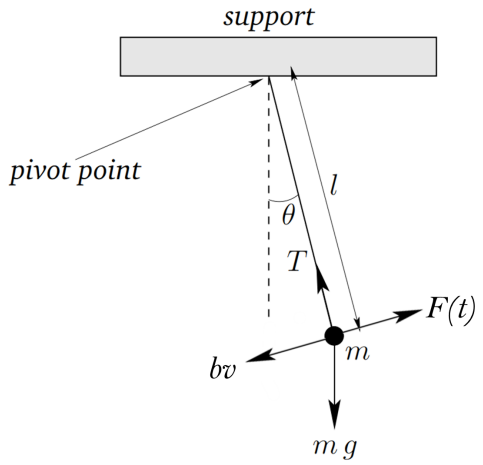

Figure 1: Forces acting on a damped-driven pendulum

The equation of motion for a damped and driven pendulum can be derived by comparing the torques and moment of inertia, $I\ddot{\theta} = \tau$, where I is the moment of inertia and τ is the net torque about the pivot yields the equation of motion for this case. In this case $I = mL^2$, since it is a point mass. The torque arises from the three forces shown in figure 1. The resistive force has magnitude bv and hence exerts a torque $-Lbv = -bL^2\dot{\theta}$. The torque of the weight is $-mgL\sin\theta$, and that of the driving force is $LF_0\cos\omega_d t$. The equation takes the form:

$$mL^2\ddot{\theta} = -bL^2\dot{\theta} - mgL\sin\theta + LF_0\cos\omega_d t$$

By dividing everything by mL^2, we get

$$\ddot{\theta} + \frac{b}{m}\dot{\theta} + \frac{g}{L}\sin\theta = \frac{F_o}{mL}\cos\omega_d t$$

This system is nonlinear due to the presence of the $\sin\theta$ term and may or may not exhibit chaotic behavior. If we approximate the system with small angles, we can linearize the equation and obtain an analytic solution. However, for the general case, an analytical solution becomes difficult to obtain. To explore the possibility of chaos, we must use the non-linear form of the equation. This three-dimensional continuous non-linear system consists of three parameters that can be varied: the driving frequency, the damping coefficient, and the driving force amplitude. The strength of the driving force can be denoted by the parameter γ, which is the ratio of the driving force amplitude to the weight of the body. The damping coefficient $\frac{b}{m}$ is taken as 2β. The term $\frac{g}{l}$ is the square of the natural frequency of the pendulum which can be denoted by w_0^2. Hence the equation of motion takes the form:

$$\ddot{\theta} + 2\beta\dot{\theta} + \omega_0^2\sin\theta = \gamma\omega_0^2\cos\omega_d t$$

The equation of motion for a damped and driven simple harmonic oscillator with a small angle approximation can also be derived. The equation takes the form:

$$\ddot{\theta} + 2\beta\dot{\theta} + \omega_0^2\theta = \gamma\omega_0^2\cos\omega_d t$$

This linear system with finite degrees of freedom does not exhibit chaotic behavior.

It can be readily observed that in absence of a driving force, the right hand side of the equation vanishes and gives us the equation of a damped pendulum. If we consider a system with no damping, the damping coefficient becomes zero and we obtain the familiar equation of the simple pendulum:

$$\ddot{\theta} + \frac{g}{L}\sin\theta = 0$$

1.2 Chaos

Chaotic behavior is observed in various situations, ranging from highly complex mechanical systems to everyday occurrences. Examples include species populations, the forced Duffing Equation, and even the

weather. The theory of chaos originated in the 1960s when a meteorologist named Edward Lorenz neglected a few decimal places while running a trial for his weather simulator.

Although there is no universally accepted formal mathematical definition of the term chaos, it can be described as the deterministic system's long-term, aperiodic behavior that exhibits sensitive dependence on initial conditions.

1.2 Dimensionality and The Poincaré Bendixson theorem

The Poincaré-Bendixson theorem says that two dimensional continuous systems cannot exhibit chaos, as trajectories in a two-dimensional plane will either converge to a fixed point or reach a stable limit cycle. However, in three-dimensional systems, trajectories can move indefinitely around the phase space, allowing for randomness and the potential for chaos to arise. As a result, chaotic behavior is only observed in continuous dynamical systems with three or more dimensions. In the absence of damping or forcing terms, a simple pendulum is a linear deterministic system that does not exhibit chaos. However, introducing a sinusoidal forcing term that depends explicitly on time and renders the differential equation nonlinear results in chaotic behavior.

1.2 Global Mixing

Global mixing is a fundamental property of chaotic dynamical systems, which arises due to the uniqueness theorem that governs the trajectories of these systems. Because trajectories cannot intersect with each other in the phase space, the trajectories of a three-dimensional chaotic system can move randomly and endlessly around the phase space without intersecting, eventually covering the entire phase space. This behavior is known as global mixing, which means that any region of the phase space overlaps with any other given region during the evolution of the system.

Global mixing is an important characteristic of chaotic systems since any small perturbation to the system's initial conditions can lead to a significant effect on its long-term behavior. The presence of global mixing is often associated with the presence of strange attractors, which are geometric objects in phase space that describe the long-term behavior of the system. Because of global mixing, chaotic systems are highly sensitive to initial conditions, making it difficult to predict their long-term behavior. Therefore, global mixing is a crucial property of chaotic systems, which renders long-term predictions impossible.

1.2 The Lyapunov Exponent

To be called chaotic, a system should show sensitive dependence on initial conditions, in the sense that neighboring orbits separate exponentially fast, on average. Given some initial condition x_0, consider a nearby point $x_0 + \delta_0$, where the initial separation δ_0 is extremely small. Let δ_n be the separation after n iterates. If $|\delta_n| \approx |\delta_0| e^{n\lambda}$, then λ is called the Lyapunov exponent. A positive Lyapunov exponent is a signature of chaos.

A more precise and computationally useful formula for λ can be derived. By taking logarithms and noting that $\delta_n = f^n(x_0 + \delta_0) - f^n(x_0)$, we obtain[1]

$$\begin{aligned}\lambda &\approx \frac{1}{n} \ln \left| \frac{\delta_n}{\delta_0} \right| \\ &= \frac{1}{n} \ln \left| \frac{f^n(x_0 + \delta_0) - f^n(x_0)}{\delta_0} \right| \\ &= \frac{1}{n} \ln \left| (f^n)'(x_0) \right|\end{aligned}$$

1. Steven Strogatz, *Nonlinear Dynamics and Chaos: With Applications to Physics, Biology, Chemistry, and Engineering* (CRC Press, 2018).

where we've taken the limit $\delta_0 \to 0$ in the last step. The term inside the logarithm can be expanded by the chain rule:

$$(f^n)'(x_0) = \prod_{i=0}^{n-1} f'(x_i).$$

Hence

$$\begin{aligned}\lambda &\approx \frac{1}{n} \ln \left| \prod_{i=0}^{n-1} f'(x_i) \right| \\ &= \frac{1}{n} \sum_{i=0}^{n-1} \ln \left| f'(x_i) \right|\end{aligned}$$

If this expression has a limit as $n \to \infty$, we define that limit to be the Lyapunov exponent for the orbit starting at x_0 :

$$\lambda = \lim_{n\to\infty} \left\{ \frac{1}{n} \sum_{i=0}^{n-1} \ln \left| f'(x_i) \right| \right\}.$$

Note that λ depends on x_0. However, it is the same for all x_0 in the basin of attraction of a given attractor. For stable fixed points and cycles, λ is negative, for chaotic attractors, λ is positive.

In certain physical scenarios, an object has the potential to escape and not return, resulting in an increase in separation distance between trajectories. For instance, if two water droplets situated on opposite sides of a continental divide flow downhill, they may move away from each other exponentially. Furthermore, some mathematical models may lead to trajectories that extend infinitely, leading to a positive Lyapunov exponent. However, this behavior is simple, and the Lyapunov exponent alone cannot be utilized to define chaos.[2]

1.2 Bifurcation Diagram

A bifurcation diagram is a graphical representation of how the behavior of a dynamic system changes as one or more parameters are changed. Specifically, it plots the long-term behavior of the system (such as the value of a particular variable) against a varying parameter, such as a control parameter or initial condition.

Bifurcation diagrams are useful in chaos theory because they can help to visualize how the behavior of a system changes as it approaches a chaotic regime. As the parameter is varied, the system may undergo a series of bifurcations, where the long-term behavior of the system suddenly changes. These bifurcations can lead to complex and unpredictable behavior, including chaotic behavior.

1.2 Poincaré Sections

In chaos theory, Poincaré sections are a powerful tool used to study the behavior of dynamical systems. They are named after the French mathematician Henri Poincaré, who first introduced the concept in his studies of the three-body problem.

A Poincaré section is a two-dimensional cross-section of a three-dimensional dynamical system. It is created by choosing a fixed value of one of the system's state variables and then plotting the values of another state variable as the system evolves over time. The resulting plot is a set of points that represent the intersections of the system's trajectory with the chosen cross-section.

In a Poincaré section, θ and ω are recorded as a single point each time the trajectory pierces through the θ-ω plane corresponding to one value of the drive phase. Thus, once per drive period, a new (θ,ω) point is added to the plot as the trajectory repeatedly pierces that particular plane.

Poincaré sections are useful because they can re-

2. *What is Chaos? Part III: Lyapunov Exponents*, https://thechaostician.com/what-is-chaos-part-iii-lyapunov-exponents/, Accessed on May 6, 2023.

veal important information about the long-term behavior of a dynamical system. For example, they can help identify periodic orbits, chaotic behavior, and other types of complex behavior that might not be immediately obvious from the system's equations or phase space plots.

1.3 Magnetic Pendulum

The pendulum consists of a magnet that is suspended by a string, with a distribution of similar magnets placed in the plane below the pendulum. The dynamics of the pendulum are affected by the number and positioning of these magnets. All magnets in the system, including the one attached to the end of the pendulum, are oriented in the same direction. As the pendulum is set in motion from different starting positions, it eventually stabilizes around one of the magnets in the plane. However, the motion of the pendulum during the intermediate period is characterized by chaotic behavior.

The experiment assumes several conditions. First, the pendulum length is much greater than the spacing between the magnets, allowing for the assumption that the pendulum bob moves in a plane rather than a sphere. Second, the magnets are positioned in a plane just below the pendulum and act as point attractors. Lastly, the magnetic forces obey an inverse squared law, meaning that the force is inversely proportional to the square of the distance between the magnets and the pendulum. These assumptions provide the necessary framework for understanding the behavior of the pendulum under the influence of the magnetic field.[3]

3. Heinz-Otto Peitgen, Hartmut Jürgens, and Dietmar Saupe, *New Frontiers of Science* (Springer-Verlag New York, Inc., 1992).

Parameters

- (x, y) : the Cartesian coordinate of the pendulum bob
- (x_i, y_i) : the Cartesian coordinates of the magnets
- d : the vertical distance from the pendulum bob to the plane in which the magnets lie.
- R : the friction force coefficient.
- C : the gravitational (spring) force coefficient

The Model

We define the origin of the Cartesian coordinate system to be the gravitational equilibrium position of the pendulum bob, and specify coordinates of the magnets relative to this origin. The distance between the pendulum bob and magnet i is

$$\sqrt{(x_i - x)^2 + (y_i - y)^2 + d^2}$$

Hence the magnetic force is proportional to

$$\frac{1}{(x_i - x)^2 + (y_i - y)^2 + d^2}$$

. However, we must ignore the vertical component of this force, as we assume the pendulum bob is restricted to a plane. Taking this into account, it can be shown that the x and y components of the force are

$$\vec{F}_x = \frac{x_i - x}{\left((x_i - x)^2 + (y_i - y)^2 + d^2\right)^{3/2}},$$
$$\vec{F}_y = \frac{y_i - y}{\left((x_i - x)^2 + (y_i - y)^2 + d^2\right)^{3/2}}.$$

The gravitational force that pulls the pendulum bob back to the origin is proportional to the distance from the origin; thus, the x and y components are proportional to $-x$ and $-y$ respectively. The friction force acts in opposition to the direction of motion and is proportional to the velocity (x', y')

Using Newton's Law, we equate the sum of the above three forces to the acceleration of the mass,

and after rearranging, we arrive at our governing equations:

$$x'' + Rx' - \sum_i \frac{x_i - x}{\left((x_i - x)^2 + (y_i - y)^2 + d^2\right)^{3/2}} + Cx = 0$$

$$y'' + Ry' - \sum_i \frac{y_i - y}{\left((x_i - x)^2 + (y_i - y)^2 + d^2\right)^{3/2}} + Cy = 0$$

1.4 Fourier Analysis

A mathematical model called Fourier Transform can be used to transform signals between two different domains, such as transforming a signal from the frequency domain to the time domain or vice versa. Many applications in Engineering and Physics use the Fourier transform. The Fourier transform can extend the Fourier series to non-periodic functions, allowing functions to be viewed as the sum of simple sinusoids. The Fourier transform is considered a generalisation of the complex Fourier series in the limit $L \to \infty$, and discrete A_n can be converted to the continuous $F(k)dk$ by letting $n/L \to k$. Finally, the sum can be converted to an integral.

Therefore, the Fourier transform of a function $f(x)$ is given by:

$$F(k) = \int_{-\infty}^{\infty} f(x) e^{-2\pi i k x} dx$$

where $F(k)$ represents the Fourier transform of $f(x)$. Similarly, the inverse Fourier transform can be represented using the following equation:

$$f(x) = \int_{-\infty}^{\infty} F(k) e^{2\pi i k x} dk$$

where $f(x)$ represents the inverse Fourier transform of $F(k)$.

These equations allow us to transform a function between the time and frequency domains, and vice versa, using the Fourier transform.
The Fourier Transform of sine and cosine functions are dirac delta functions. Therefore, when we take the Fourier Transform of x_1 and x_2, we are expected to get peaks at f_1 corresponding to ω_1 for in-phase oscillation, f_2 corresponding to ω_2 for out of phase oscillation and both f_1 and f_2 for beats and arbitrary initial conditions.

Fourier Series

Any Periodic function can be expressed as the sum of a sever of sines and cosines of different amplitudes → A function $f(x)$ can be expressed as a series of sines and cosines as:

$$f(x) = \frac{1}{2}a_0 + \sum_{n=1}^{\infty} a_n \cos(nx) + \sum_{n=1}^{\infty} b_n \sin(nx)$$

Where,

$$a_0 = \frac{1}{\pi}\int_{-\pi}^{\pi} f(x)dx$$

$$a_n = \frac{1}{\pi}\int_{-\pi}^{\pi} f(x)\cos(nx)dn$$

$$b_n = \frac{1}{\pi}\int_{-\pi}^{\pi} f(n)\sin(nx)dn \ldots \quad (n = 1, 2, 3 \ldots)$$

Fourier Transform is basically the transformation of any periodic function into the Fourier Series.

Fast Fourier Transform

It's an important measurement method in the science of audio and acoustics measurement. It converts a signal into individual spectral components and thereby provides frequency information about the signal.
This is the same which we used to get the oscillation frequencies for various initial conditions of this experiment.
Fast Fourier Transform, as clear from its name, is the algorithm to compute "discrete fourier transforms" (DFT) of a sequence or its inverse with a high speed of computation. In other words, number of operations for evaluate the DFT.s is required very less in FFT algorithm
If we wish to find the frequency spectrum of a function that we have, the continuous Fourier transform

is not so useful, so we need to have the Discrete version of Fourier transform.

Forward DFT:

$$F_n = \sum_{k=0}^{N-1} f_k e^{-2\pi i n k/N}$$

The complex numbers $f_0, f_1 \dots f_N$ are transformed to complex numbers $F_0, F_1 \dots F_N$.

Inverse DFT

$$f_k = \frac{1}{N} \sum_{n=0}^{N-1} F_n e^{-2\pi i k n/N}$$

$$F_0, F_1 \dots F_N \longrightarrow f_0, f_1 \dots f_N$$

$\Rightarrow$ Let $x_0, x_1 \dots x_{N-1}$ be complex numbers, the DFT is defined by the formula,

$x_k = \sum_{n=0}^{N-1} x_n e^{-i2\pi k n/N} \quad \{k = 0, L, \dots . N - L\}$.

Evaluating x_k directly requires $O\left(N^2\right)$ operations: there will be N output of x_k. Each output further requires a sum of N terms.

Then, FFT is the method to compute the same results for x_k in $O(N \log N)$ operations.

Clearly, $(N \log N) << \left(N^2\right)$ hence its preferable .

2 Methodology

2.1 Experimental Setup and Procedure

2.1 Simple Pendulum

A simple pendulum experiment was conducted in a laboratory setting. A small bob was attached to a light string, which was in turn suspended from a pivot point. The pendulum was set into motion by pulling the bob to one side and releasing it. The motion of the pendulum was recorded using a video camera, and later analyzed using tracker software to obtain data for further analysis. The experiment was conducted for four different amplitudes: 4 degrees, 10 degrees, 20 degrees, and 30 degrees. However, the videos for amplitudes of 4 degrees and 20 degrees were used for the analysis, as the video for the 30 degree amplitude was not able to be tracked using the software and was therefore discarded.

Precautions

- The thread should be light
- The point of suspension should be reasonably rigid
- The pendulum should oscillate in the vertical plane without any spin motion
- The amplitude of vibration should be small
- There must not be any strong wind blowing during the experiment.

2.1 Magnetic Pendulum

The experiment involves modifying the simple pendulum setup by incorporating magnets to induce oscillations. A free-moving pendulum capable of nearly spherical motion is used. The bob of the pendulum is attached with a magnet and three magnets of equal strength are placed at a short distance below the bob. After setting the bob into motion, a video of the trajectory is recorded from the top to capture the entire motion. The recorded video is then analyzed using the Tracker software, and the obtained data is utilized for further analysis to demonstrate the occurrence of chaos in the system.

Precautions

- Make sure that the magnet is securely mounted to the pendulum.

- Keep all magnetic materials away from the experimental setup to avoid interfering with the pendulum's motion.
- Use only low power magnets and avoid using strong magnets to prevent the pendulum from getting stuck.
- Ensure that the pendulum has enough clearance to swing freely without hitting any nearby objects.

2.2 Simulation

The simulation and plotting of graphs were done using the Python programming language. Additionally, the NumPy library was utilized to perform a Fourier transform using the "fft" function. In order to integrate the damped driven pendulum, the fourth-order Runge-Kutta method (RK4) was applied. In order to calculate the Lyapunov exponent, we had two separate arrays containing values of theta for different driving amplitudes. Each of these arrays belonged to a different stability regime, and γ values were calculated for each one. To determine the difference between theta values, θ_1 and θ_2 were subtracted and the absolute value was taken to ensure only positive values were stored. For the bifurcation diagram, an array was created to represent a range of driving amplitudes. A loop was used to calculate the corresponding theta and omega values for each gamma value. These values were then plotted against the driving amplitude to generate the bifurcation plot required. An array of driving amplitudes was defined for a model, and corresponding values of ϑ and ω were calculated for each amplitude. Specific values of θ and ω were sampled out using the definition of Poincaré space, with sampling occurring every 10th element due to a time-period of one and step-length of 0.1, by using a nested loop. The sampled values of θ and ω were stored in two different arrays and were converted to the appropriate domain. These arrays were then plotted against each other to create a sampled out phase portrait that defined the Poincaré section for the system.

2.2 Fourth-Order Runge Kutta Method

The fourth order Runge-Kutta Method (RK-4) was utilized to obtain the solution of the second order differential equation, which represents the equation of motion in the project. The Euler method was not used as it has higher truncation errors and is less numerically stable. The RK-4 method integrates the function symmetrically, in contrast to the asymmetric nature of the Euler method. The algorithm for the RK-4 integrator is as follows[4] :

- The values of k are calculated at the mid-point of each step as follows,

$$\begin{aligned} k_1 &= hf\left(t_i, x_i\right) \\ k_2 &= hf\left(t_i + \frac{h}{2}, x_i + \frac{k_1}{2}\right) \\ k_3 &= hf\left(t_i + \frac{h}{2}, x_i + \frac{k_2}{2}\right) \\ k_4 &= hf\left(t_i + h, x_i + k_3\right) \end{aligned}$$

- The value of y_{i+1} is calculated using the above values of k as follows,

$$y_{i+1} = y_i + \frac{1}{6}k_1 + 2k_2 + 2k_3 + k_4$$

The step-length h is defined by the user, and the error for an n^{th} order RK-4 method can be approximated as $\epsilon = \frac{n}{h} + h^n$. The minimum step length h_0 and the associated error ϵ_0 can be approximated as $h_0 \sim \eta^{\frac{1}{(n+1)}}$ and $\epsilon_0 \sim \eta^{\frac{n}{(n+1)}}$, respectively. By applying the RK-4 method, errors in the intermediate steps are canceled out, resulting in an error that is of the fourth order of the original error.

4. Richard Fitzpatrick, "Computational physics" (Lecture notes, University of Texas at Austin, 2006).

3 Results

3.1 Experimental

3.1 Simple Pendulum

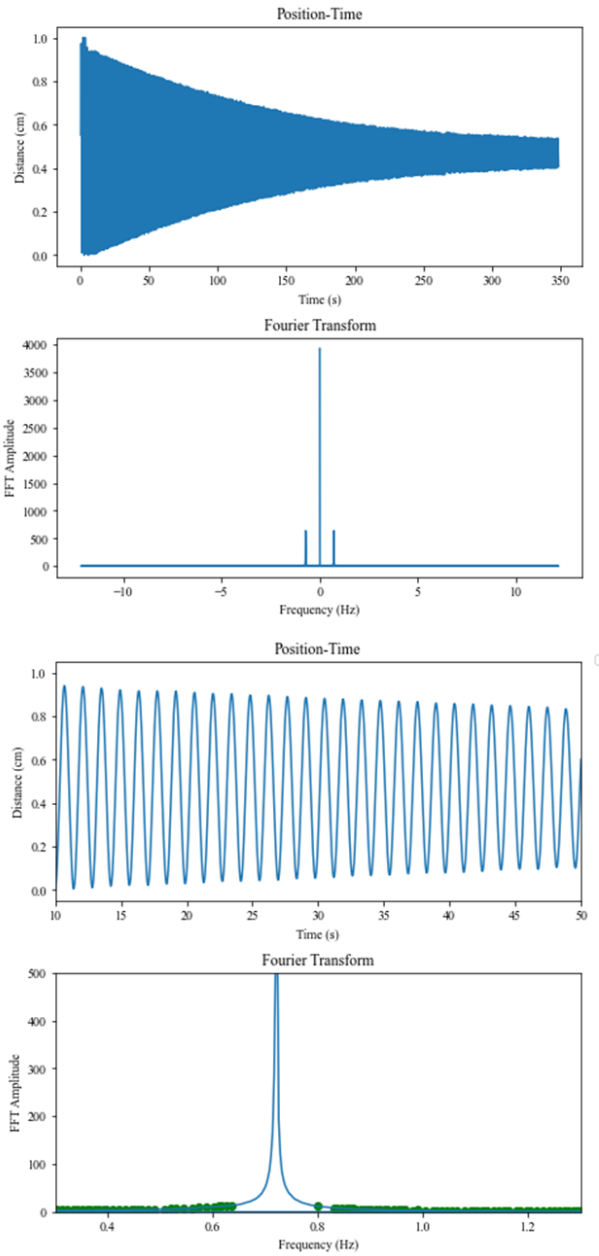

Figure 2: The Position-Time Graph for the Simple Pendulum with Amplitude 4^o and the Fourier Transform of it with a peak at frequency $\nu = \frac{\omega}{2\pi} = 0.7$ Hz which is the natural frequency of the pendulum.

The 3rd and 4th graphs are the relevantly zoomed in versions of the 1st and 2nd graphs respectively. The position-time graph in Figure 2 reveals that the pendulum used in the lab is not a simple pendulum, but a damped pendulum due to the presence of damping forces, such as air resistance, and other factors. The amplitude of oscillation continuously decreases over time. From now on in this report, whenever the term "simple pendulum" is used, it refers to a damped pendulum.

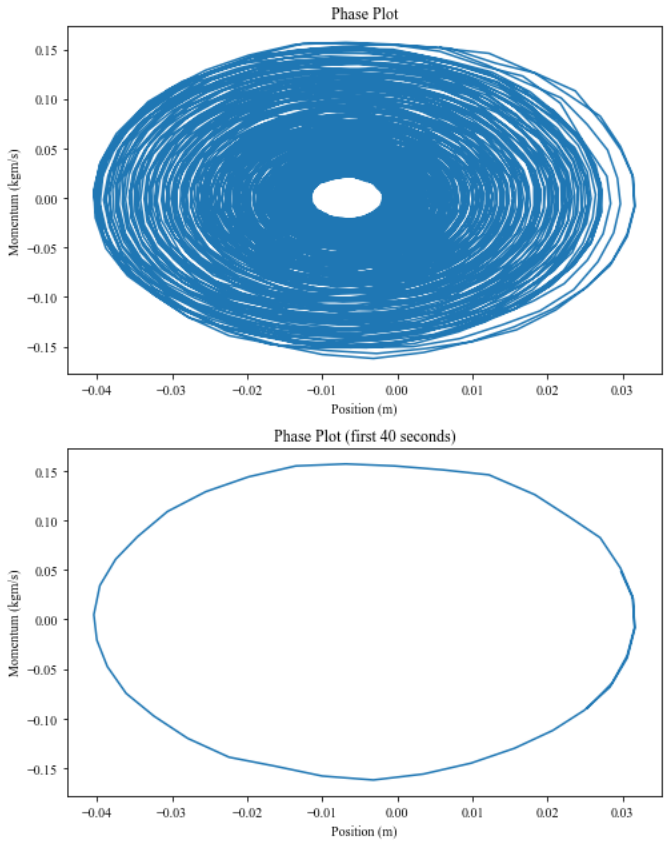

Figure 3: 2D Phase Space Plot for pendulum with amplitude 4^o

The phase plot for the pendulum also reveals that the pendulum is actually a damped pendulum as the phase space curve is an inward closing spiral which approaches the origin as time goes to infinity. The pendulum eventually stops due to the damping forces. The second curve shows just one cycle of oscillation from where the nature of the phase space curve is more evident and this is the curve that we are expected to get for an ideal simple pendulum. As this graph is plotted only for one cycle, the effect

of damping is not seen and we get the ellipse that we expected to get for a simple pendulum

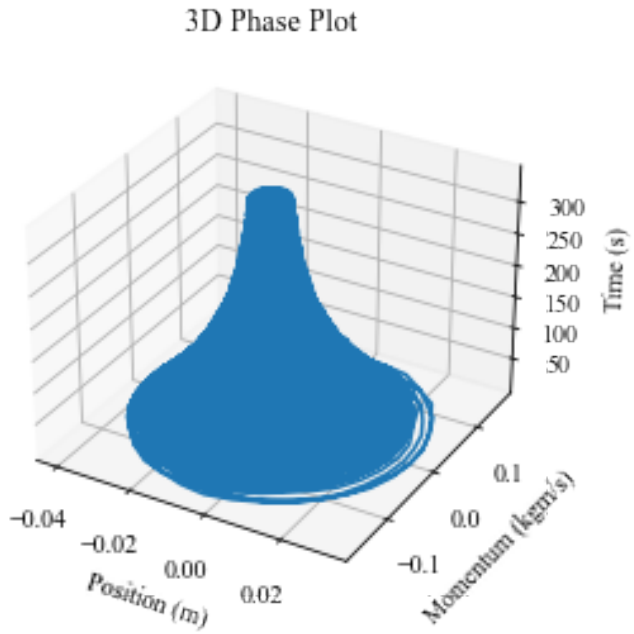

Figure 4: 3D Phase Space Plot for pendulum with amplitude 4^o

This is also a Phase Space plot for the same pendulum but it has been plotted in 3D so that we can get a glimpse at the time evolution of the phase space trajectory.

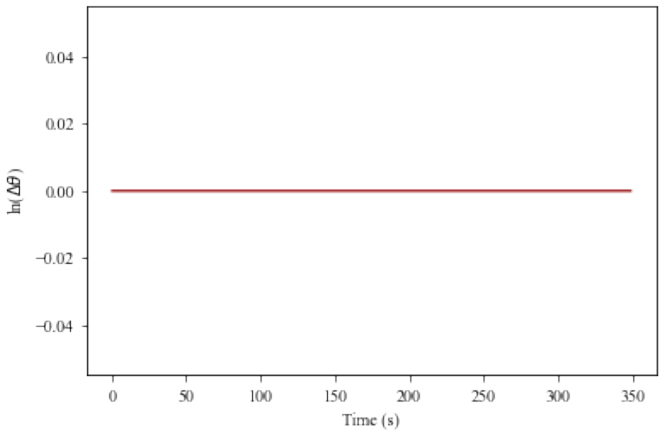

Figure 5: Deviation of Trajectories with respect to time in the pendulum with amplitude 4^o

As expected, for a simple pendulum, the trajectories do not deviate with time and slight difference in initial conditions doesn't make a difference to the late-time behaviour of the system. This shows that the simple pendulum is a non-chaotic system.

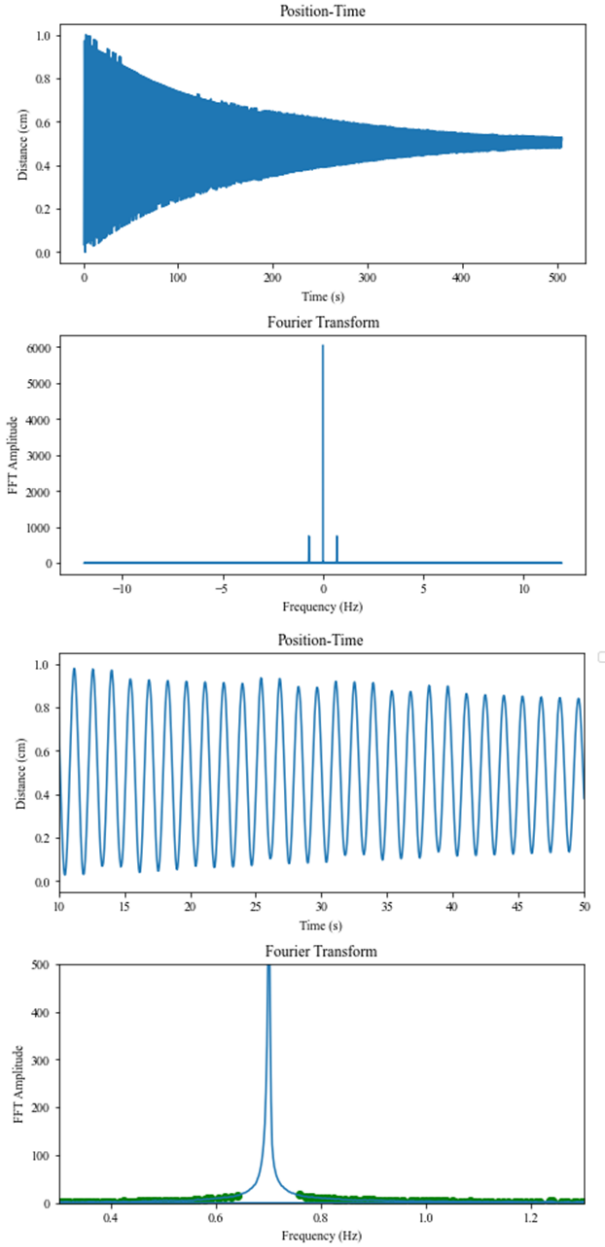

Figure 6: The Position-Time Graph for the Simple Pendulum with Amplitude 20^o and the Fourier Transform of it. The Fourier Transform gives a peak at frequency $\nu = 0.7$ Hz which is the natural frequency of the pendulum. The 3rd and 4th graphs are the relevantly zoomed in versions of the 1st and 2nd graphs respectively.

Comparing figure 6 with 2 we realise that changing the amplitude from 4^o to 20^o doesn't make much of a difference in the system. The peak of Fourier

Transform is obtained at the same frequency as expected because it is the natural frequency of the system.

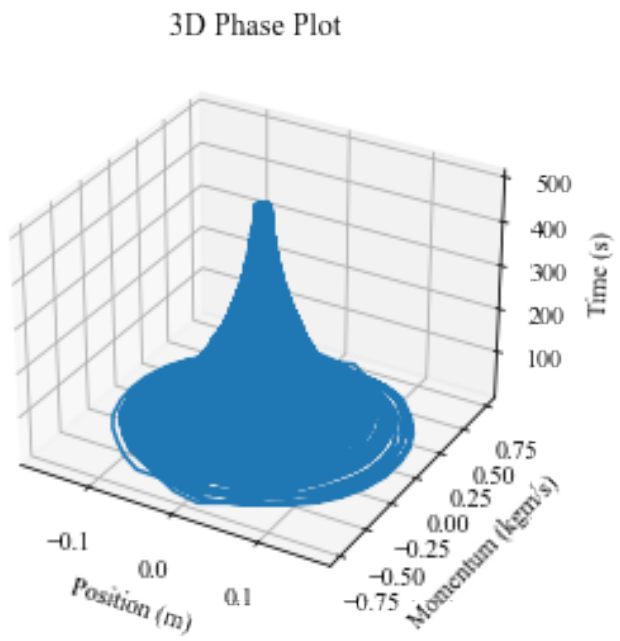

Figure 7: 2D Phase Space Plot for pendulum with amplitude 20^o

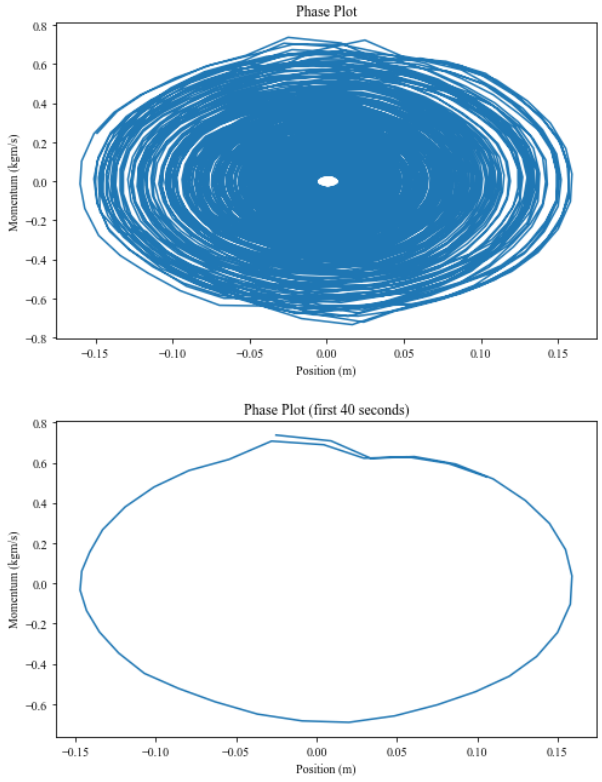

Figure 8: 3D Phase Space Plot for pendulum with amplitude 20^o

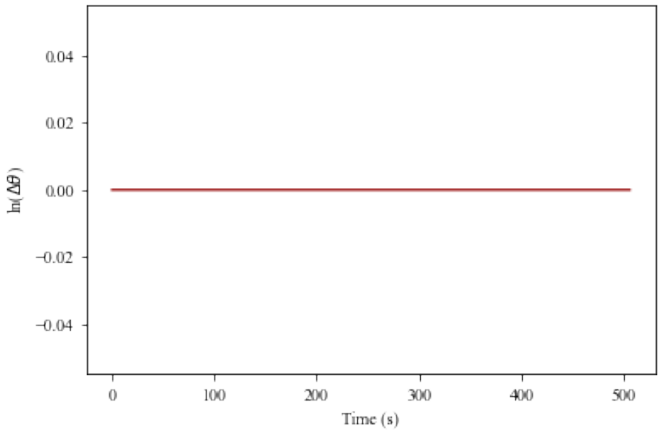

Figure 9: Deviation of trajectories with respect to time in the pendulum with amplitude 20^o

The rest of the results obtained from the pendulum with amplitude 20^o is the same as the pendulum with with amplitude 4^o. It would've been interesting to vary the amplitude more and look for non-linearity and anharmonicity in the system. Although the small-angle approximation is generally considered to be true only till 4^o, the above results demonstrate that there isn't much difference even when the amplitude is 5 times that.

3.1 Magnetic Pendulum

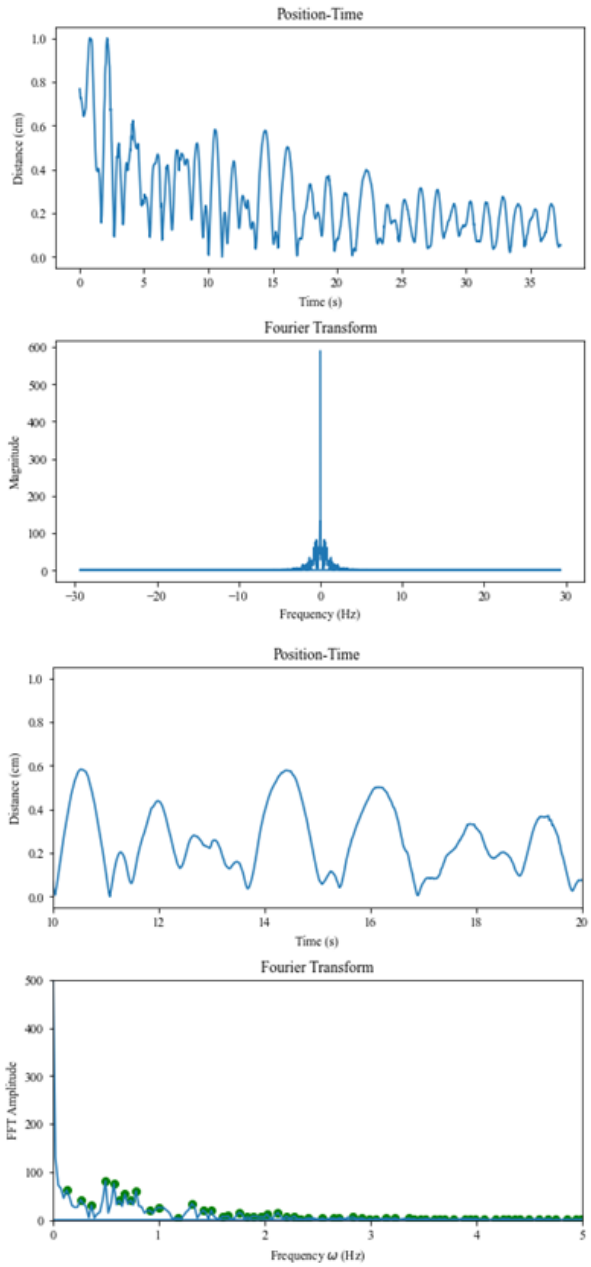

Figure 10: Position-Time Graph of the Magnetic Pendulum along with its Fourier Transform. The 3rd and 4th graphs are the relevantly zoomed in versions of the 1st and 2nd graphs respectively.

We can see that the position-time graph of the magnetic pendulum does not show harmonicity or any particular pattern which might indicate the presence of chaos in this system but the position-time graph does not give a definitive answer and further analysis is needed. It is also observed that the system does not peak at any particular frequency but has multiple peaks which indicates that the pendulum is subject to additional forces or nonlinearities that make its motion more complex and non-harmonic.

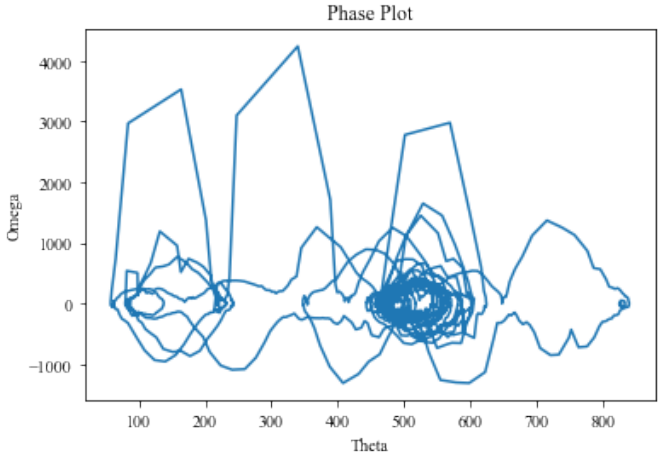

Figure 11: 2D Phase Space Plot for Magnetic Pendulum

From the phase space plot we can see that the curve is not restricted to any particular region but is filling up a large part of the phase space indicating global mixing. It is also noticed that the phase space trajectories are crossing so a 3D plot of the Phase Space is plotted to see if there is any discrepancy.

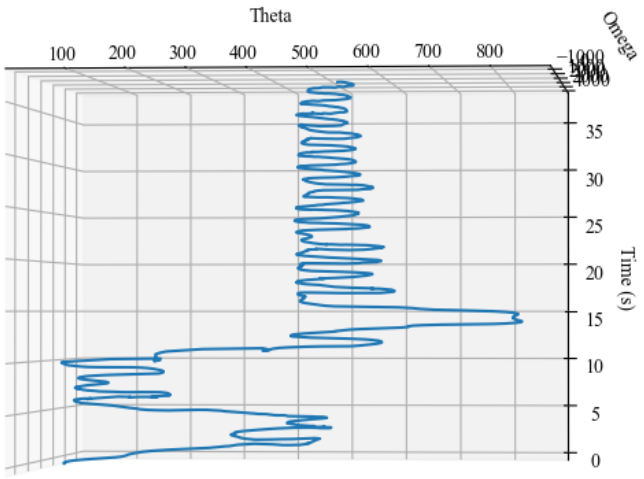

Figure 12: 3D Phase Space Plot for Magnetic Pendulum

The 3D Phase Space Plot reveals that the tra-

jectories are not crossing in phase space indicating that the system has more degrees of freedom in 3D and can exhibit more complex behavior. In 3D phase space, the trajectories are able to move around each other or avoid each other due to the additional degrees of freedom, while in 2D phase space, the trajectories are more constrained and forced to cross.

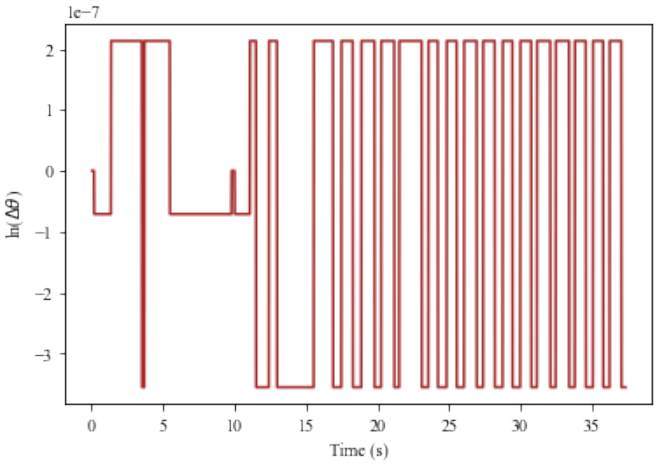

Figure 13: Deviation in Trajectories with respect to time

It is observed that the trajectories deviate in time indicating the presence of chaotic behaviour. More claritiy is obtained after plotting the lyapunov exponent with time.

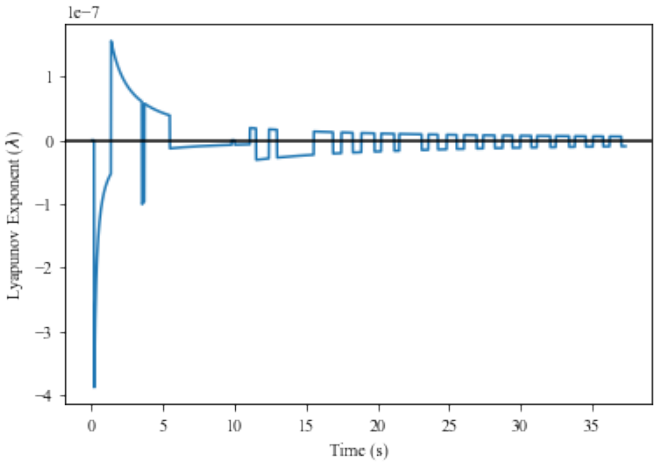

Figure 14: Lyapunov Exponent Versus Time

When the lyapunov exponent is greater than zero, it indicates that the trajectories are diverging and that the system might be chaotic. The system is initially stable as it is pulled away from the magnets. Once it interacts with the magnets, it exhibits chaotic behaviour. After that it keeps on oscillating between chaotic and stable tendencies as its distance from the magnet changes and the system comes to a stop after losing energy due to damping.

3.2 Simulation

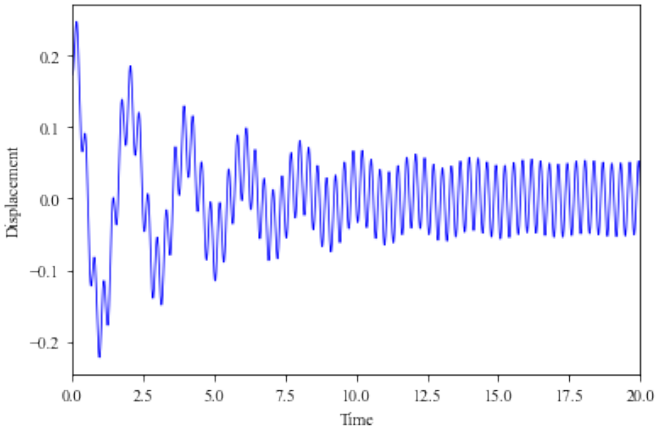

Figure 15: Position-Time Graph for $\gamma = 0.5, F_0 = 20, \omega_d = 20,$

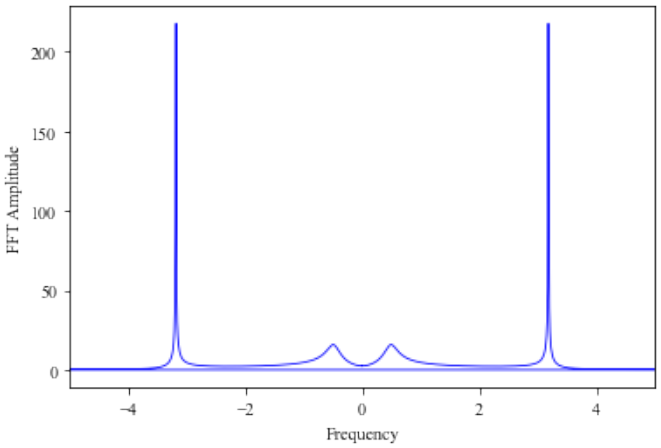

Figure 16: Fourier Transform of Position-Time Graph for $\gamma = 0.5, F_0 = 20, \omega_d = 20$

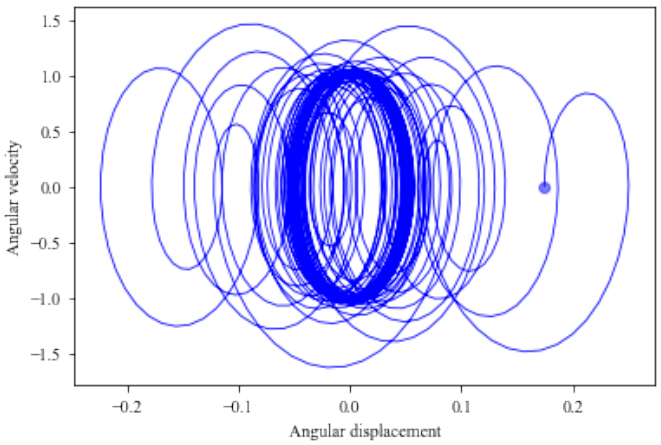

Figure 17: 2D Phase Space Plot Graph for $\gamma = 0.5, F_0 = 20, \omega_d = 20$

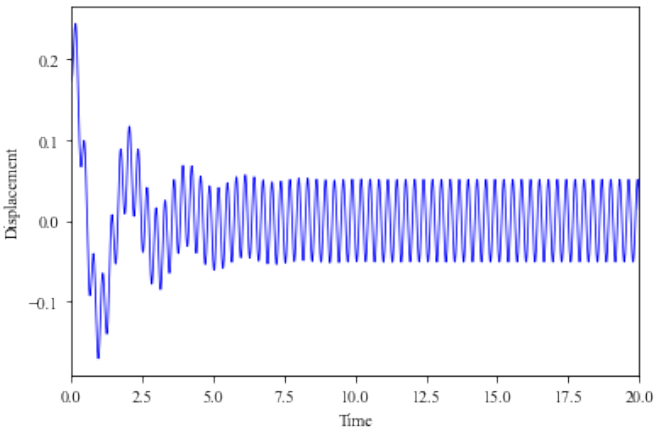

Figure 19: Position-Time Graph for $\gamma = 1.2, F_0 = 20, \omega_d = 20$

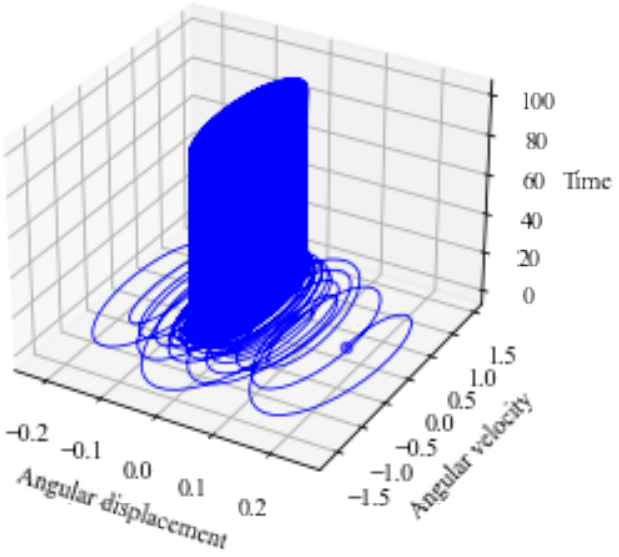

Figure 18: 3D Phase Space Plot Graph for $\gamma = 0.5, F_0 = 20, \omega_d = 20$

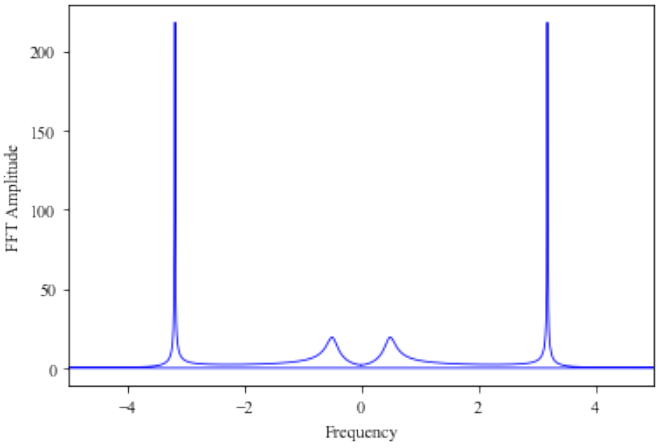

Figure 20: Fourier Transform of Position-Time Graph for $\gamma = 1.2, F_0 = 20, \omega_d = 20$

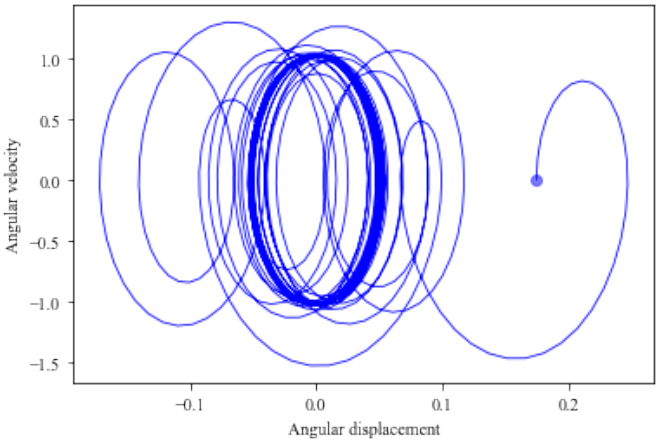

Figure 21: 2D Phase Space Plot Graph for $\gamma = 1.2, F_0 = 20, \omega_d = 20$

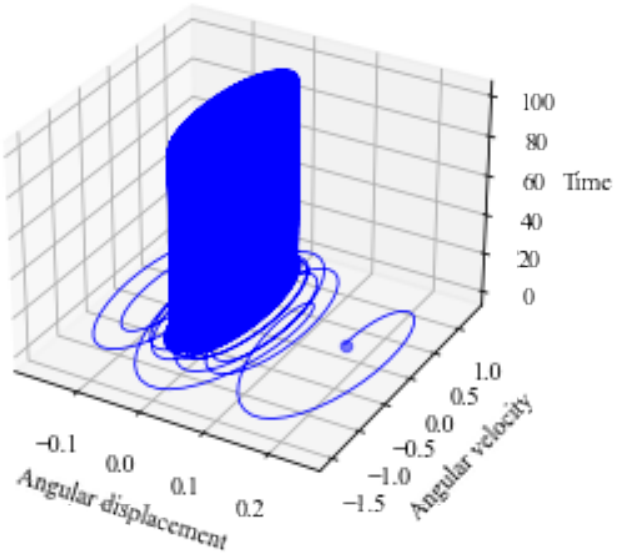

Figure 22: 3D Phase Space Plot Graph for $\gamma = 1.2, F_0 = 20, \omega_d = 20$

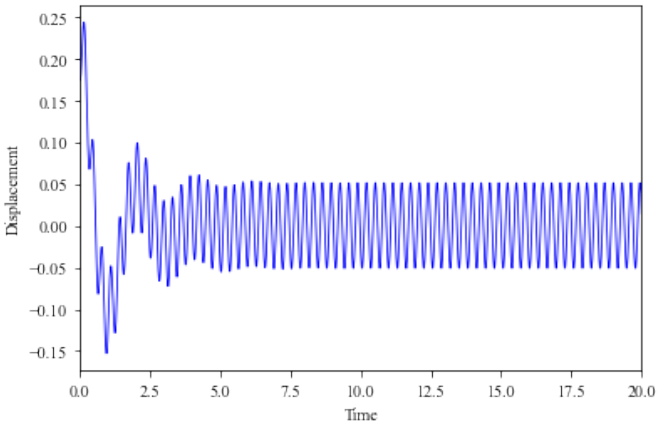

Figure 23: Position-Time Graph for $\gamma = 1.5, F_0 = 20, \omega_d = 20$

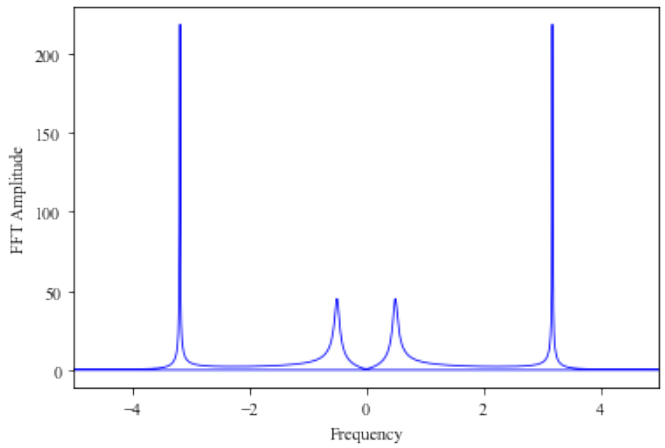

Figure 24: Fourier Transform of Position-Time Graph for $\gamma = 1.5, F_0 = 20, \omega_d = 20$

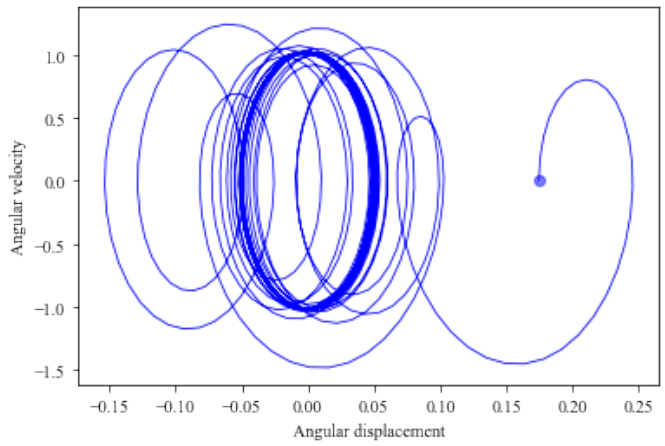

Figure 25: 2D Phase Space Plot Graph for $\gamma = 1.5, F_0 = 20, \omega_d = 20$

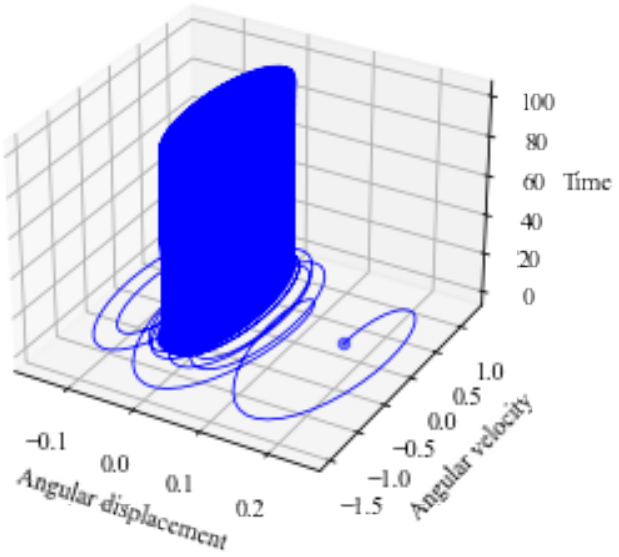

Figure 26: 3D Phase Space Plot Graph for $\gamma = 1.5, F_0 = 20, \omega_d = 20$

In all the above plots we observe that the position-time graphs have a very clear transient state followed by a steady state where the driving frequency dominates. It is also noticed that if the value of γ is lower, it takes more time for the system to reach its steady state. For the chosen initial conditions, all the systems tend to approach limit cycles in long time in their phase space plots. This is easier to understand from the 3D phase space plots where it is observed that the systems tend to be chaotic towards the beginning but eventually become stable. The Fourier Transforms of all the position-time graphs are also plotted to check the natural frequency of the system and in each case there is a peak at 3.18 Hz indicating that it is the natural frequency of the system. To understand the chaotic behaviour of the three systems better, we plot the lyapunov exponent vs. time graphs for the systems for the first 20 seconds as the systems tend to enter a steady state after that.

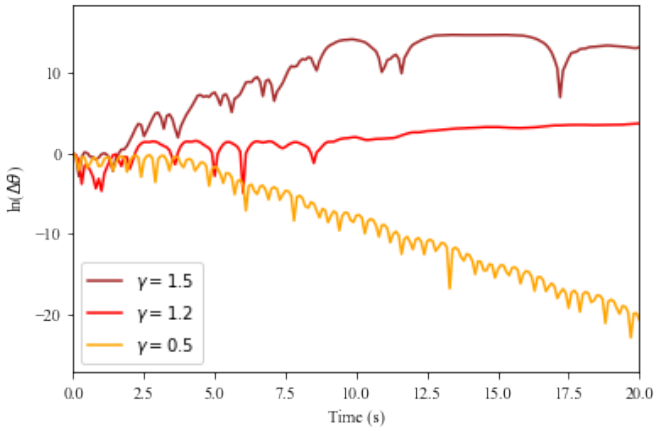

Figure 27: Plot showing deviation of trajectories with respect to time, to study the nature of Lyapunov exponent in both chaotic and stable regimes for $F_0 = 20, \omega_d = 20$

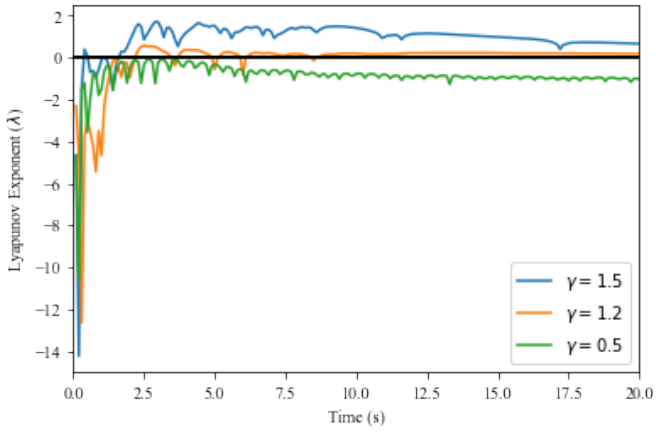

Figure 28: Plot showing the change in Lyapunov exponent with time for different driving amplitudes for $F_0 = 20, \omega_d = 20$

From the Lyapunov exponent vs. Time plots, we observe that for $\gamma = 1.5$, the value of lyapunov exponent is positive indicating that the trajectories are diverging and that the system is chaotic. For $\gamma = 1.2$ the trajectories do not diverge much and lyapunov exponent is close to zero indicating stability. For lower values of $\gamma = 0.5$, the system is definitely non-chaotic as the value of lyapunov exponent is negative. As the value of the γ is low, the system reaches the stable state soon as the driving frequency dominates. We will look at the stable and

chaotic conditions in details later for slightly different initial conditions to obtain interesting results.

But, before that we try using arbitrarily high values of γ, F_0, ω_d to observe the results we obtain. Observing the above plots, we might have thought that the chaos in the system would increase if we keep on increasing the value of γ because the value of the lyapunov exponent became negative to positive as we varied γ from 0.5 to 1.5 but it is not always the case.

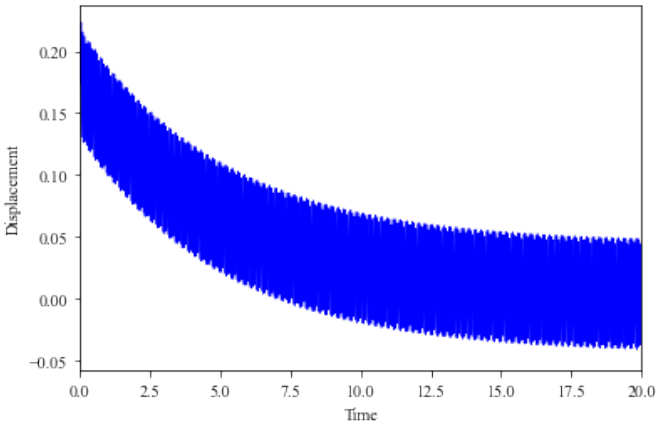

Figure 29: Position-Time Graph for $\gamma = 50, F_0 = 500, \omega_d = 100$

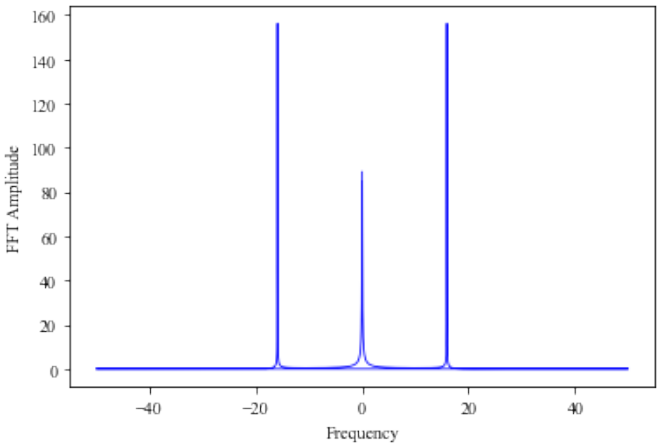

Figure 30: Fourier Transform of Position-Time Graph for $\gamma = 50, F_0 = 500, \omega_d = 100$

From the above Fourier-Transform Plot we obtain the natural frequency of the system as 15.92 Hz.

If the values of F_0, ω_d had been the same as the previous cases, we would've obtained the same value of natural frequency, 3.18.

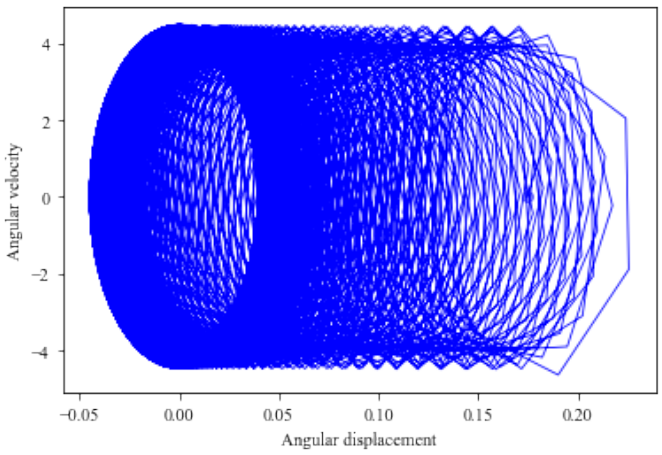

Figure 31: 2D Phase Space Plot for $\gamma = 50, F_0 = 500, \omega_d = 100$

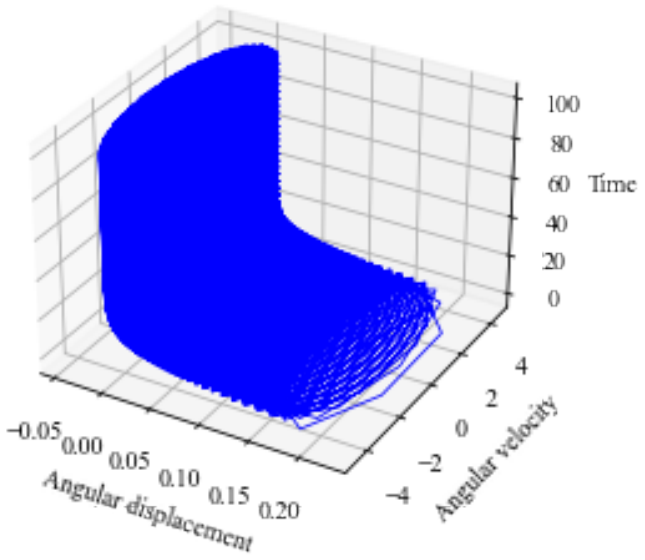

Figure 32: 3D Phase Space Plot for $\gamma = 50, F_0 = 500, \omega_d = 100$

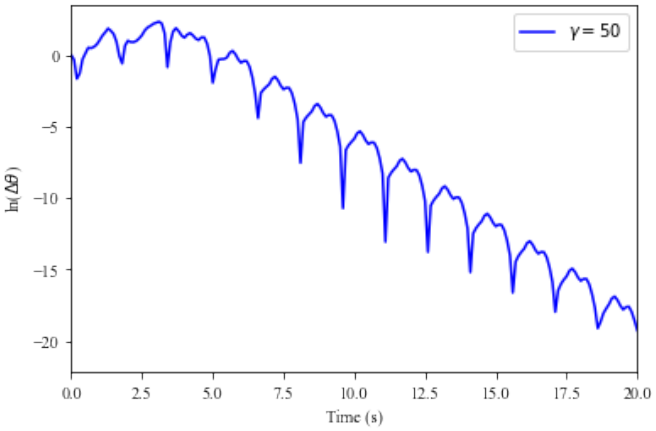

Figure 33: Plot showing deviation of trajectories with respect to time for $\gamma = 50, F_0 = 500, \omega_d = 100$

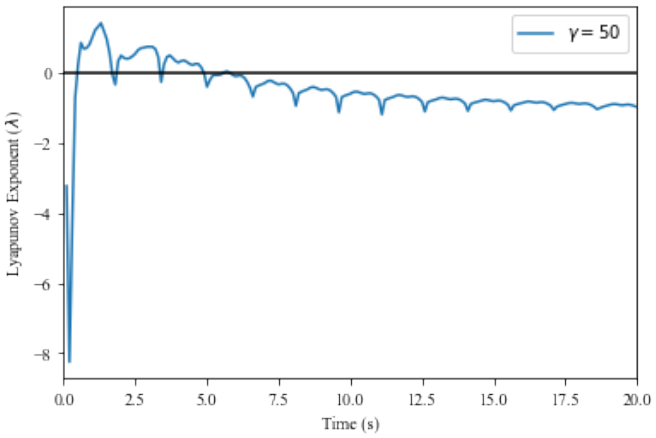

Figure 34: Plot showing the change in Lyapunov exponent with time for $\gamma = 50, F_0 = 500, \omega_d = 100$

From the above plots we see that for a very high value of $\gamma = 50$, the lyapunov exponent remains positive only for a very short time and the system becomes stable very soon and shows a clear pattern as observed from the phase plots also. In fact, this system is less chaotic than the previous system with $\gamma = 1.5$. To get a complete understanding of this, we need to plot the bifurcation diagram of the system. The bifurcation diagram will tell us for which values of γ the system will be chaotic and when it will be stable. As demonstrated by the above examples, it is generally not a simple and easily predictable relation.

A different set of initial conditions is chosen for the Bifurcation diagram and the poincaré sections but the same values of γ are considered.

Parameter	**Value**
Natural Frequency (ω_0)	5π
Damping Factor (β)	$\frac{5\pi}{4}$
Driving Frequency (ω_d)	2π
Steady-State Time Period (τ)	1
Step-Length (h)	0.1
Initial Angular Displacement (θ_0)	0
Initial Angular Velocity (ω)	0

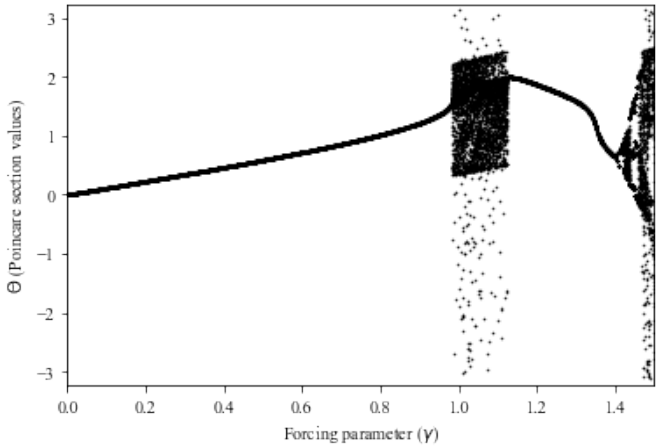

Figure 35: The bifurcation diagram for the chaotic pendulum with initial conditions $\omega_0 = 5\pi, \beta = \frac{\omega_0}{4}, \omega_d = 2\pi$

The spread states signify chaos while the discrete packets of points mark the idea of order. The bifurcation has two types of distinct regions. There are regions that resemble vertical lines. These are regions where there are points that are almost continuously scattered vertically, for instance, the region $0 < \gamma < 1$ and $1.15 < \gamma < 1.4$. The other regions exhibit regions of chaos.

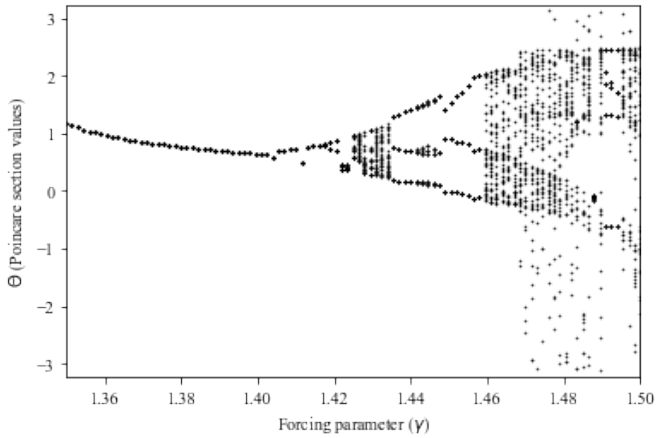

Figure 36: Zoomed in bifurcation diagram for the chaotic pendulum with initial conditions $\omega_0 = 5\pi, \beta = \frac{\omega_0}{4}, \omega_d = 2\pi$ in the region $1.35 < \gamma < 1.5$

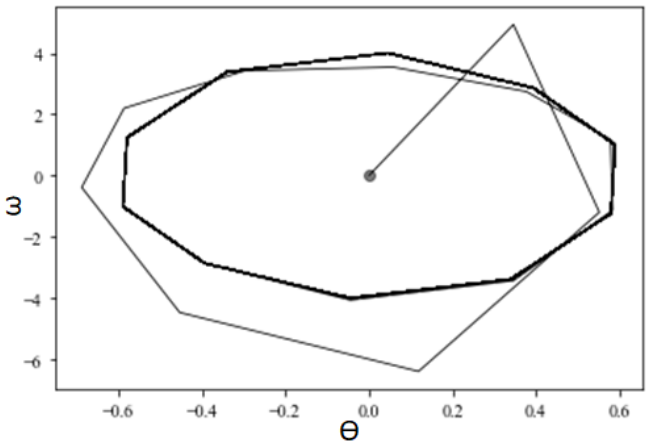

Figure 37: The plot shows that the system reaches a stable limit cycle in its late time behaviour for $\gamma = 0.5$

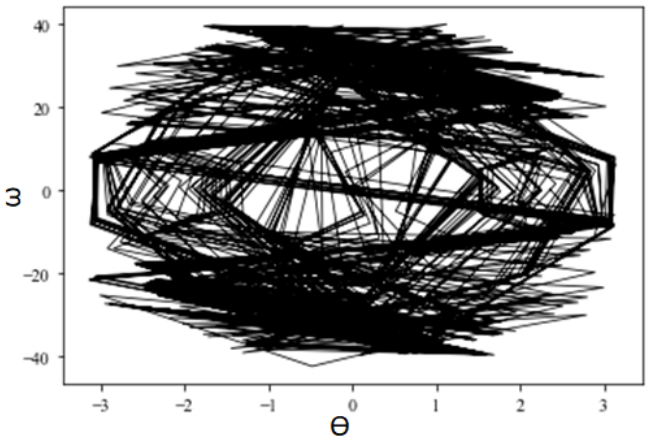

Figure 38: The plot shows that the system shows global mixing in its late time behaviour for $\gamma = 1.5$

In the zoomed in bifurcation diagram we can see that around $\gamma = 1.435$, the system splits into three segments indicating period tripling. In a period tripling bifurcation, the period of the pendulum's oscillation changes from a single, stable value to three different values, each corresponding to a different type of motion. Specifically, the pendulum's motion alternates between periods of three different oscillation amplitudes, with each period lasting for three times the duration of the previous period. This behavior is known as "period-3" behavior. Period tripling is a type of chaotic behavior that can arise in certain types of nonlinear systems, including damped driven pendulums. It is characterized by a lack of predictability in the pendulum's motion, as small changes in the initial conditions of the system can lead to drastically different outcomes. If we zoom in further, we will notice many more such details which indicates that the system does not repeat its behaviour. Hence, the damped driven pendulum is a system that exhibits chaos.

Plotting the phase space plots for the $\gamma = 0.5$ and $\gamma = 1.5$, we obtain global mixing for $\gamma = 1.5$ as the system is chaotic for that value of γ and as expected, we obtain a stable limit cycle for $\gamma = 0.5$ as the system is non-chaotic for that value of γ.

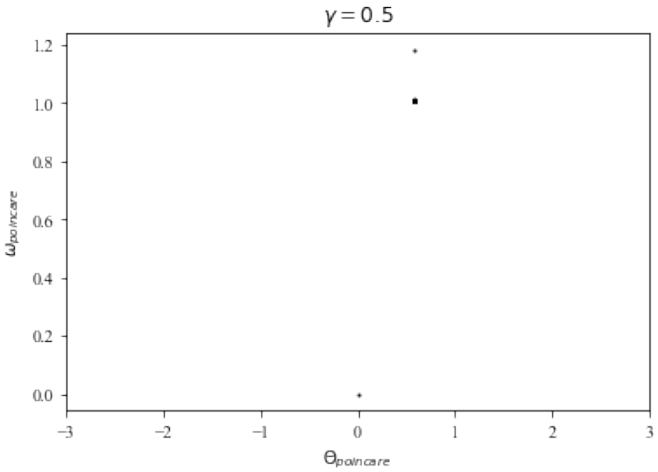

Figure 39: Poincaré Section for $\gamma = 0.5$

As for $\gamma = 0.5$ the system is not chaotic, we get a few closely spaced points for the poincaré section indicating once again that the system is stable.

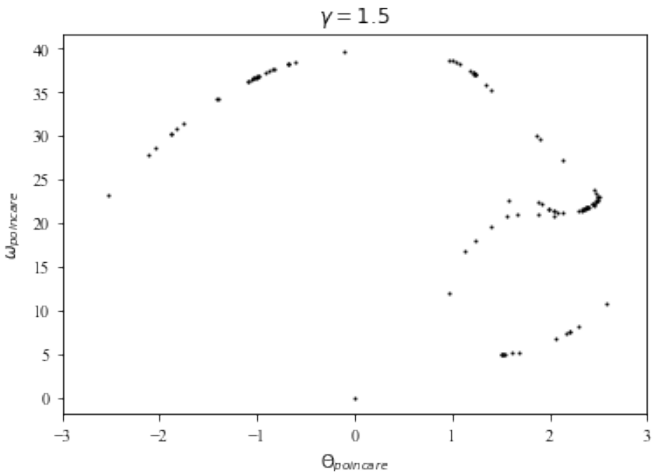

Figure 40: Poincaré Section for $\gamma = 1.5$

For $\gamma = 1.5$, we get a bunch of points in the poincaré section spread widely and the distribution is random indicating chaos.

4 Conclusion

In this paper, an analysis of the simple pendulum and the magnetic pendulum was conducted using Fourier transforms and Lyapunov exponents. The findings suggest that the simple or damped pendulum is not chaotic for small amplitudes, while the magnetic pendulum exhibits chaotic behavior. Additionally, the non-linear dynamics of the damped-driven pendulum were studied without the linear approximation using an RK4 integrator. The system demonstrates characteristics of chaos for certain values of the driving force parameter γ, with evidence of exponential sensitivity to initial conditions, diverging phase portrait trajectories, and a positive Lyapunov exponent. A period tripling and chaos were observed in the bifurcation diagram, and the Poincaré section confirms the chaotic nature of the system.

5 Discussion

5.1 Future Scope of Study

- Obtaining the poincaré sections for different values of γ to observe fractals.
- Studying Chaos in different kinds of Coupled Pendula systems and by changing different parameters like the length, masses of the bobs etc.
- Carrying out a more detailed experimental study of the magnetic pendulum, finding basins of attraction
- Studying the effect of strength of the magnet on chaotic behaviour
- Considering the possibility of chaos by changing 2β, i.e., damping factor.
- Considering a non-linear damping dependence, i.e., $F_{friction} \propto v^2$ and studying the possibility of chaos

5.2 Limitations

Although one of the objectives of this paper was to experimentally study the dynamics of the simple pendulum, it was not possible due to damping in the motion of the pendulum. Therefore, the dynamics of an undriven damped pendulum were essentially studied. However, for the position-time graphs and phase space plots, specific portions were zoomed in to demonstrate the results a simple pendulum would yield.

Although a positive value of the Lyapunov exponent is indicative of a chaotic system, our graphs for the magnetic pendulum show that at times, the Lyapunov exponent does become negative. This is because the experimental setup used small magnets of low strength, and only three magnets were used in the experiment, resulting in a small area of influence for the magnets. As a result, when the trajectory of the pendulum bob was outside the area of magnet influence, the system exhibited non-chaotic motion, moving solely under the influence of gravity and the restoring force. Therefore, the bob exhibited chaotic behavior only when it was in proximity to the magnets, indicating that the magnetic force induces chaos in the system, making the magnetic pendulum a chaotic system.

Certain sharp turns are observed in some of our graphs. In the case of the simple and magnetic pendulum, these turns are attributed to the time resolution of the tracker software, which has a particular least count. The videos for the magnetic pendulum are much shorter, which accentuates the sharp turns. For the simulated graphs, a time step of 0.1 was used, but ideally, a time step of 0.01 should have been used to reduce errors. However, this was avoided due to the significant computational power required, and using a large time step contributed to errors. With a better processor, a smaller time step could have been chosen, resulting in more accurate results.

6 Appendices

Raw Data and Python Code

7 References

Cline, David. "Variational Principles in Classical Mechanics: Nonlinear Systems and Chaos," 2019. Accessed May 10, 2023. https://phys.libretexts.org/Bookshelves/Classical_Mechanics/Variational_Principles_in_Classical_Mechanics_(Cline)/04%3A_Nonlinear_Systems_and_Chaos.

Fitzpatrick, Richard. "Computational physics." Lecture notes, University of Texas at Austin, 2006.

Madangarli, Anjali, Nitin Jha, and Spandan Pandya. *The Dynamics of the Chaotic Pendulum*. May 2022.

Mika. "Angle Transformation To $[-\pi, \pi]$," 2022. Accessed May 10, 2023. https://mika-s.github.io/python/control-theory/kinematics/2017/12/18/transformation-to-pipi.html.

Peitgen, Heinz-Otto, Hartmut Jürgens, and Dietmar Saupe. *New Frontiers of Science*. Springer-Verlag New York, Inc., 1992.

Strogatz, Steven. *Nonlinear Dynamics and Chaos: With Applications to Physics, Biology, Chemistry, and Engineering*. CRC Press, 2018.

What is Chaos? Part III: Lyapunov Exponents. https://thechaostician.com/what-is-chaos-part-iii-lyapunov-exponents/. Accessed on May 6, 2023.